

Analysis of the immunological biomarker profile during acute Zika virus infection reveals the overexpression of CXCL10, a chemokine already linked to neuronal damage

Short Title: CXCL10 overexpression in Acute Zika Virus Infection

Felipe Gomes Naveca^{1,2¶*}, Gemilson Soares Pontes^{3&}, Aileen Yu-hen Chang^{4&}, George Allan Villarouco da Silva^{2,7}, Valdinete Alves do Nascimento¹, Dana Cristina da Silva Monteiro², Marineide Souza da Silva², Lígia Fernandes Abdalla^{2,5}, João Hugo Abdalla Santos⁶, Tatiana Amaral Pires de Almeida¹, Matilde del Carmen Contreras Mejía¹, Tirza Gabrielle Ramos de Mesquita⁷, Helia Valeria de Souza Encarnação⁷, Matheus de Souza Gomes⁸, Laurence Rodrigues Amaral⁸, Ana Carolina Campi-Azevedo⁹, Jordana Graziela Coelho-dos-Reis⁹, Lis Ribeiro do Vale Antonelli⁹, Andréa Teixeira-Carvalho^{9&}, Olindo Assis Martins-Filho^{9¶*}, Rajendranath Ramasawmy^{7,10}

1 Programa de Pós-Graduação em Biologia da Interação Patógeno-Hospedeiro, Instituto Leônidas e Maria Deane – Fiocruz Amazônia, Manaus, Amazonas, Brazil

2 Programa de Pós-Graduação em Imunologia Básica e Aplicada, Universidade Federal do Amazonas, Manaus, Amazonas, Brazil

3 Instituto Nacional de Pesquisas da Amazônia, Manaus, Amazonas, Brazil

4 George Washington University, Washington, DC, United States of America

5 Universidade do Estado do Amazonas, Manaus, Amazonas, Brazil

6 Hospital Adventista de Manaus, Manaus, Amazonas, Brazil

7 Fundação de Medicina Tropical – Dr Heitor Vieira Dourado, Manaus, Amazonas, Brazil

8 Universidade Federal de Uberlândia, Patos de Minas, Minas Gerais, Brazil

9 Centro de Pesquisas René Rachou – Fiocruz Minas, Belo Horizonte, Minas Gerais,
Brazil

10 Universidade Nilton Lins, Manaus, Amazonas, Brazil

* felipe.naveca@fiocruz.br (FGN)

* oamfilho@cpqrr.fiocruz.br (OAMF)

[¶]These authors contributed equally to this work.

[&]These authors also contributed equally to this work.

1 **Abstract**

2 Infection with Zika virus (ZIKV) manifests in a broad spectrum of disease ranging from
3 mild illness to severe neurological complications. To define immunologic correlates of
4 ZIKV infection, we characterized the levels of circulating cytokines, chemokines and
5 growth factors in 54 infected patients of both genders, at five different time-points after
6 symptoms onset using microbeads multiplex immunoassay; statistical analysis and data
7 mining compared to 100 age-matched controls. ZIKV-infected patients present a
8 striking systemic inflammatory response with high levels of pro-inflammatory
9 mediators. Despite the strong inflammatory pattern, IL-1Ra and IL-4 are also induced
10 during acute infection. Interestingly, the inflammatory cytokines, IL-1 β , IL-13, IL-17,
11 TNF- α , IFN- γ ; chemokines, CXCL8, CCL2, CCL5; and the growth factor G-CSF
12 display a bimodal distribution accompanying viremia. While this is the first manuscript
13 to document bimodal distributions of viremia in ZIKV infection, bimodal viremia has
14 been documented in other viral infections with primary viremia peaks during mild
15 systemic disease and a secondary viremia with distribution of the virus to organs and

16 tissues. Moreover, biomarker network analysis demonstrated distinct dynamics in
17 consonance with the bimodal viremia profiles at different time-points during ZIKV
18 infection. Such robust cytokine and chemokine response has been associated with
19 blood-brain barrier permeability and neuroinvasiveness in other flaviviral infections.
20 High-dimensional data analysis further established CXCL10, a chemokine involved in
21 fetal neuron apoptosis and Guillain-Barré syndrome, as the most promising biomarker
22 of acute ZIKV infection for a potential clinical application.

23

24 **Author Summary**

25 Infection with Zika virus manifests in a broad spectrum of disease ranging from mild
26 illness to severe neurological complications. This study characterized the levels of
27 circulating cytokines, chemokines and growth factors in Zika-infected patients showing
28 an inflammatory immune response. Specifically, this study identified a chemokine,
29 CXCL10, known to be involved in fetal neuron apoptosis and Guillain-Barré syndrome,
30 as the most promising biomarker to characterize acute Zika virus infection.

31

32 **Introduction**

33 The Zika virus (ZIKV) is an arthropod-borne *Flavivirus*, transmitted mainly by the bite
34 of female *Aedes* mosquitos, that usually causes a mild illness characterized by
35 conjunctivitis, pruritus, muscle and joint pain, rash and slight fever [1]. Outbreaks of
36 ZIKV infection were first recorded in Micronesia and later in French Polynesia, where
37 atypical manifestations were initially documented, including the Guillain-Barré
38 Syndrome [2,3]. In Brazil, ZIKV infection during pregnancy was linked to an unusual
39 increase in the number of microcephaly cases [4]. Following the Brazilian report of
40 congenital malformations, the number of microcephaly cases in French Polynesia were

41 reanalyzed, and a connection with ZIKV was further established [5]. The broad
42 spectrum of fetal clinical manifestations resulting from ZIKV infection lead to a new
43 classification termed Zika Congenital Syndrome [6].
44 Host immune response plays an important role in the clinical course of patients with
45 viral infection. Particularly, cellular immunity and key components of the innate
46 immune response, such as interferons and other cytokines/chemokines, play an essential
47 role in limiting the viral spread [7]. To date, only two studies describing immune
48 mediators in Zika-infected patients have been reported [8,9]. In Tappe et al, reliable
49 immunological biomarker profile during acute infection could not be established due to
50 the small sample size. Kam et al. describes immune markers from a cohort from
51 Campinas, Brazil showing inflammatory immune response and several immune
52 mediators specifically higher in ZIKV-infected patients, with levels of CXCL10, IL-10, and
53 HGF differentiating between patients with and without neurological complications. Kam et
54 al. also found higher levels of CXCL10, IL-22, MCP-1, and TNF- α were observed in
55 ZIKV-infected pregnant women carrying babies with fetal growth associated
56 malformations.
57 In this study, we evaluated the immune response during the acute ZIKV infection by
58 analysis the serum levels of cytokines, chemokines and growth factors from an adult
59 cohort from Manaus, Brazil of 54 ZIKV-infected cases and 100 controls over five time
60 points during symptomatic ZIKV infection. We present the time course of cytokine
61 response in relation to viremia and identify a chemokine that may serve as a biomarker
62 of acute ZIKV infection, providing new insights into ZIKV neuropathogenesis.

63

64 **Methods**

65 **Study Population and Design**

66 We used a non-probabilistic convenience sampling and a cross-sectional experimental
67 design, together with robust statistical analysis and data mining, for the evaluation of
68 the immunological biomarker profile during acute ZIKV infection. In the first semester
69 of 2016, a total of 54 suspected ZIKV-infected cases (29 non-pregnant females and 25
70 males, all adults) were recruited at Hospital Adventista de Manaus, Amazonas state,
71 Brazil. All patients presented a maculopapular rash, with or without fever, and at least
72 one of the following symptoms: pruritus, arthralgia, joint swelling or conjunctival
73 hyperemia, within five days after the symptoms onset. Age-matched non-infected (NI)
74 controls, females (46) and males (54), were enrolled for comparison and basic
75 characteristics, including physical examination and virological findings are provided.
76 Comprehensive laboratory records were available for 21 patients (15 male and six
77 female), including routine laboratory tests.

78

79 **Ethics Statement**

80 The study protocol was approved by the Ethics Committee of the Universidade do
81 Estado do Amazonas (CAAE: 56745116.6.0000.5016) and all subjects included
82 provided written informed consent.

83

84 **Differential molecular diagnosis of Zika and viral load estimative**

85 Serum samples were sent to Fiocruz Amazônia and tested for ZIKV (envelope coding
86 region) [10], Chikungunya (CHIKV) [11] and Dengue (DENV) [12] by RT-qPCR.
87 Samples positive for CHIKV or DENV were excluded. Sample inclusion criteria also
88 required the internal control (spiked MS2 bacteriophage) to display a Ct value between
89 30-32. The viremia was indirectly estimated by RT-qPCR and reported as $1/Ct*100$.

90

91 **Dengue virus serology**

92 Serum samples were tested for previous exposure to DENV with Serion ELISA classic
93 Dengue Virus IgG (Institut Virion/Serion GmbH, Germany).

94

95 **Microbeads assay for serum biomarkers**

96 High-performance microbeads 27-plex assay (Bio-Rad, Hercules, CA, USA) was
97 employed for detection and quantification of multiple targets, including: CXCL8 (IL-8);
98 CXCL10 (IP-10); CCL11 (Eotaxin); CCL3 (MIP-1 α); CCL4 (MIP-1 β); CCL2 (MCP-
99 1); CCL5 (RANTES); IL-1 β , IL-6, TNF- α ; IL-12; IFN- γ , IL-17; IL-1Ra (IL-1 receptor
100 antagonist); IL-2; IL-4; IL-5; IL-7; IL-9; IL-10; IL-13; IL-15; FGF-basic; PDGF;
101 VEGF; G-CSF and GM-CSF. Samples were tested according to the manufacturer's
102 instructions on a Bio-Plax 200 instrument (Bio-Rad). The serum levels of IL-2, IL-7,
103 and IL-15 were below the detection limits in several samples and were excluded of
104 further analysis. The results were expressed as pg/mL.

105

106 **Statistical analysis and Data mining**

107 Statistical analyses were initially performed using GraphPad Prism (GraphPad Software
108 6.0, San Diego, CA, USA). Outliers within each measurement group were identified by
109 the ROUT Method (Q=1%) and removed. Cleaned data was then used for the evaluation
110 of Gaussian distribution with D'Agostino & Pearson omnibus normality test.
111 Comparative analysis of the clinical records was carried out by Fisher's exact test. The
112 analysis of biomarker levels between NI controls *vs.* ZIKV-infected cases, and between
113 genders, was performed by Mann-Whitney test. Multivariate correlations for biomarker
114 levels and routine laboratory tests were analyzed with the nonparametric Spearman's

115 test (alpha 0.05) running on the JMP Software, v13.1.0 (SAS Institute, Cary, NC, USA).
116 Correlations (Spearman ρ) were represented by a color map matrix.
117 The dynamics of viremia, chemokines, cytokines and growth factors were evaluated
118 using the median value of each analyte. Comparative analysis of the biomarkers was
119 carried out by Kruskal-Wallis followed by Dunn's post-test. For all tests, significant
120 differences were considered at two-tailed $p < 0.05$.
121 Data management strategies were applied to identify general and time-specific profiles.
122 Biomarker signature analysis was carried out as previously described [13]. Radar charts
123 were assembled to compile the biomarker signature of NI controls and ZIKV-infected
124 cases applying the 75th percentile as threshold. Venn diagram scrutiny was carried out to
125 identify attributes, along with the timeline of the symptoms onset
126 <http://bioinformatics.psb.ugent.be/webtools/Venn/>. Cytoscape software v3.2.0
127 (<http://www.cytoscape.org/>) was employed for visualizing and integrating multiple
128 attributes into circular nodal networks. Connecting edges were drawn to underscore the
129 association as positive (solid line) or negative (dashed line). The biomarker cluster
130 pattern was defined by heatmaps assembled using R software (heatmap.2 function;
131 v3.0.1). Decision tree algorithms were generated with WEKA software v3.6.11
132 (University of Waikato, New Zealand) to identify root and branch attributes,
133 segregating patients from controls. ROC curves were built to define the cut-off and
134 biomarkers with better performance to discriminate ZIKV-infected patients from NI
135 controls. Performance indices (co-positivity, co-negativity, positive and negative
136 likelihood ratio) were calculated using the MedCalc software v7.3 (Ostend, Belgium).

137

138 **Results**

139 **Demographics, clinical records and virological data**

140 The 54 Brazilian Zika cases, 29 non-pregnant females (median age 38 years, IQR 27.5 –
141 46.5) and 25 males (median age 37 years, IQR 30 – 50), were enrolled between the first
142 and the fifth day after the symptoms onset. A group of 100 non-infected control subjects
143 who were residents of Manaus, Amazonas, Brazil were also included (46 females
144 (median age 28 years, IQR 23 – 36) and 54 males (median age 29.5 years, IQR 23 –
145 36)). The median viremia expressed as $1/Ct \times 100$ was 2.9 (min=2.7; max=4.2; IQR: 2.8
146 – 3.0). The frequency of specific ZIKV symptoms was similar between men and woman
147 with the only exception that men had increase frequency of fever compared to woman
148 (100% versus 67%, $p=0.005$) (Table 1). The DENV IgG testing showed that 94.4%
149 (51/54) of the patients were positive; two had an undetermined result and one male
150 subject was negative.

151

152 **Table 1.** Demographical aspects, clinical records and virological status
153 of ZIKV-infected patients

Parameters	All	Females	Males	p
Non-infected controls				
n	100	46	54	NA
Age (years)	29.0 (23-36)	28.0 (23-36)	29.5 (23-36)	0.58
ZIKV-infected patients				
n	54	29	25	n.a.
Age (years)	37.5 (29-48)	38.0 (27.5-46.5)	37.0 (30-50)	0.79
Days of symptoms onset	2.5 (2-4)	2.0 (1-4)	3.0 (2-4)	0.32
Rash	95.0%	94.4%	95.5%	1.00
Fever	85.0%	66.7%	100.0%	0.005
Myalgia	82.5%	83.3%	81.8%	1.00
Conjunctival hyperemia	75.0%	66.7%	81.8%	0.30

Pruritus	70.0%	66.7%	72.7%	0.73
Headache	65.0%	66.7%	63.6%	1.00
Arthralgia	60.0%	72.2%	50.0%	0.20
Joint swelling	25.0%	33.3%	18.2%	0.30
Vomiting or nausea	25.0%	33.3%	18.2%	0.30
Diarrhea	17.5%	27.8%	9.1%	0.21
Lymphadenopathy	12.5%	11.1%	13.6%	1.00
Viremia	2.9 (2.8-3.0)	2.9 (2.8-3.0)	2.9 (2.8-3.0)	0.86

154 Data are reported as median and Interquartile Range (IQR) for age, days of symptoms
155 onset and viremia. Statistical differences were assessed by Mann-Whitney test.
156 Comparative analysis of clinical records observed in females and males was carried out
157 by Fisher's exact test. Significant differences were considered at $p < 0.05$ for
158 comparisons between females vs males and are underscored by **bold/underlined**
159 format. Viremia is expressed as $1/Ct * 100$ as described in material and methods. "NA"=
160 not applicable.

161

162 **Correlation of immunological biomarkers during acute ZIKV infection with** 163 **routine laboratory tests**

164 The results of 45 continuous variables including immunological biomarkers; routine
165 laboratory tests; age; viremia and symptoms onset were analyzed (Fig 1). Overall,
166 moderate correlations were observed for several variables, whereas the strongest
167 correlations were observed between $TNF-\alpha$ and CCL5 (Spearman ρ 0.8245) and
168 Lymphocytes (%) and Neutrophils (%) (Spearman ρ -0.8084). All results were
169 represented in a color map matrix, where statistically supported associations ($p < 0.05$),
170 regarding the routine laboratorial tests and immunological biomarkers, were highlighted
171 (inserted table in Fig 1).

172

173 **Fig 1. Immunological biomarkers correlations with the results of routine**
174 **laboratorial tests, age, viremia, and symptoms.** The nonparametric Spearman's test
175 was applied to evaluate multiple correlations between immunological biomarkers and
176 the results of routine laboratorial tests. A color map matrix was plotted showing the
177 strength and direction of these correlations (-1 blue, to +1 red). Strongly supported
178 correlations ($p < 0.05$) between immunological biomarkers and routine tests are
179 highlighted in the inserted table.

180

181 **ZIKV-infected patients display high levels of circulating biomarkers**

182 Elevated levels of pro-inflammatory cytokines (IL-1 β , IL-6, TNF- α , IFN- γ and IL-17,
183 except IL-12 that was higher in controls), chemokines (CXCL8, CCL11, CCL3, CCL4,
184 CCL2, CCL5 and CXCL10) and growth factors (FGF-basic, PDGF, VEGF, G-CSF and
185 GM-CSF) were found in ZIKV-infected cases (Fig 2, light gray panels), whereas higher
186 levels of IL-5 and IL-13 in controls (Fig 2, dark gray panels). Interestingly, the levels of
187 IL-4 and IL-1Ra were also higher among patients. No differences were observed for the
188 IL-9 and IL-10 (Fig 2, white panels). A similar pattern was observed when results were
189 stratified by gender, although infected males presented significant lower levels of
190 CCL3, CCL4, CCL5, IL-17, FGF-basic and GM-CSF. No significant differences were
191 observed between female and male controls (Table 2).

192

193 **Fig 2. Panoramic Overview of Serum Chemokines, Cytokines and Growth Factors**

194 **Early After Zika Virus Infection in Adults.** Serum biomarkers (CXCL8, CCL11,
195 CCL3, CCL4, CCL2, CCL5, CXCL10, IL-1 β , IL-6, TNF- α , IL-12, IFN- γ , IL-17, IL-
196 1Ra, IL-4, IL-5, IL-9, IL-10, IL-13, FGF-basic, PDGF, VEGF, G-CSF and GM-CSF)
197 were measured in Zika virus-infected patients (ZIKV= ■, n=54) and non-infected

198 subjects (NI= □, n=100) by high performance Luminex 27-plex assay as described in
 199 methods. Data expressed as pg/mL are displayed in box and whiskers (10-90 percentile)
 200 plots. Comparative analysis between NI vs. ZIKV was performed by Mann-Whitney test
 201 and significant differences at $p < 0.05$ underscored by connecting lines. Colored
 202 backgrounds highlighted increased (light gray), decreased (dark gray) and unaltered
 203 (white) levels of serum biomarkers in ZIKV as compared to NI.

204

205 **Table 2. Serum Chemokines, Cytokines and Growth Factors Early After**
 206 **Zika Virus Infection in Adult Females and Males**

Analytes	Females (F), n=29		p (1)	Males (M), n=25		p (2)	p (3)	Score ZIKV/NI	
	NI	ZIKV		NI	ZIKV			(F)	(M)
CXCL8	0.87 (0.54-1.67)	2.26 (1.57-3.26)	0.0001	0.98 (0.70-1.93)	2.30 (1.19-3.11)	0.0018	0.5669	2.6	2.3
CCL11	16.44 (9.29-22.22)	48.94 (30.12-61.91)	0.0001	16.65 (10.62-25.20)	43.82 (29.11-56.95)	0.0001	0.3488	3.0	2.6
CCL3	0.59 (0.41-0.86)	1.15 (0.80-1.32)	0.0001	0.65 (0.45-1.13)	0.89 (0.67-1.07)	0.0469	0.0205	1.9	1.4
CCL4	7.28 (4.56-12.20)	28.76 (18.76-35.67)	0.0001	5.94 (3.75-9.79)	20.18 (12.63-26.64)	0.0001	0.0162	4.0	3.4
CCL2	2.08 (1.00-4.97)	20.73 (13.45-34.70)	0.0001	2.46 (1.94-7.15)	21.98 (11.86-32.34)	0.0001	0.9862	10.0	8.9
CCL5	15.17 (11.36-34.98)	82.77 (64.75-108.00)	0.0001	17.00 (9.83-25.70)	34.06 (23.66-65.81)	0.0001	0.0001	5.5	2.0
CXCL10	232 (128-434)	71,219 (32,899-148,407)	0.0001	218 (109-392)	44,645 (10,423-69,757)	0.0001	0.1030	307	205
IL-1β	0.52 (0.24-0.96)	0.93 (0.56-1.19)	0.0176	0.52 (0.29-1.00)	0.77 (0.61-1.14)	0.1511	0.5374	1.8	1.5
IL-6	0.29 (0.20-0.57)	0.79 (0.63-1.00)	0.0001	0.28 (0.21-0.55)	0.81 (0.52-1.73)	0.0001	0.1944	2.7	2.9
TNF-α	9.76 (6.10-20.20)	35.87 (25.45-44.08)	0.0001	10.08 (6.45-22.62)	26.93 (15.02-41.84)	0.0015	0.1101	3.7	2.7
IL-12	1.26 (0.51-2.30)	0.63 (0.22-1.66)	0.0554	1.39 (0.96-2.17)	0.34 (0.09-1.08)	0.0001	0.1895	0.5	0.2
IFN-γ	14.97 (9.63-24.54)	31.91 (26.39-38.65)	0.0001	19.79 (14.14-27.31)	26.41 (23.61-35.97)	0.0035	0.4283	2.1	1.3
IL-17	3.84 (2.21-7.53)	7.88 (6.28-9.02)	0.0001	3.57 (2.50-6.76)	5.96 (4.41-7.15)	0.0114	0.0092	2.1	1.7
IL-1Ra	11.81 (7.81-28.66)	47.00 (34.03-65.59)	0.0001	12.33 (8.95-36.13)	54.94 (30.77-115.10)	0.0001	0.3623	4.0	4.5
IL-4	0.27 (0.20-0.39)	0.81 (0.59-0.86)	0.0001	0.26 (0.17-0.41)	0.73 (0.53-0.90)	0.0001	0.6890	3.0	2.8
IL-5	3.16 (1.67-5.02)	1.50 (0.40-1.61)	0.0001	4.70 (2.00-5.35)	1.38 (1.07-1.61)	0.0001	0.5792	0.5	0.3

IL-9	2.21 (1.19-4.11)	3.10 (1.69-5.72)	0.0783	2.62 (1.59-4.69)	1.42 (1.18-3.83)	0.0837	0.0518	1.4	0.5
IL-10	1.73 (0.75-3.39)	2.11 (1.65-3.22)	0.1046	1.95 (1.51-3.02)	2.25 (1.52-3.41)	0.5478	0.9571	1.2	1.2
IL-13	0.75 (0.37-1.34)	0.48 (0.22-0.57)	0.0135	0.98 (0.80-1.57)	0.57 (0.37-0.57)	0.0001	0.3634	0.6	0.6
FGF-basic	1.84 (1.01-3.14)	<u>4.34</u> (3.71-5.27)	0.0001	2.24 (1.28-3.73)	<u>3.24</u> (2.13-4.24)	0.0468	0.0014	2.4	1.4
PDGF	359 (125-585)	1,012 (616-1,933)	0.0001	258 (196-403)	823 (416-1,578)	0.0001	0.3670	2.8	3.2
VEGF	2.87 (1.78-6.29)	6.72 (4.18-16.33)	0.0001	3.70 (2.17-4.97)	6.26 (3.66-15.21)	0.0005	0.5668	2.3	1.7
G-CSF	1.86 (1.04-2.86)	5.96 (4.43-8.05)	0.0001	1.83 (1.19-3.29)	4.94 (3.42-7.66)	0.0001	0.2400	3.2	2.7
GM-CSF	0.87 (0.52-2.00)	<u>3.76</u> (3.03-4.64)	0.0001	1.35 (0.54-2.16)	<u>2.88</u> (1.73-3.91)	0.0003	0.0256	4.4	2.1

207 Data are reported as median levels (IQR) in pg/mL. Statistical analysis was performed by Mann-
 208 Whitney test and significance reported as p(1), p(2) and p(3) values for comparisons between NI vs
 209 ZIKV females, NI vs ZIKV males and ZIKV females vs ZIKV males, respectively. Significant
 210 differences between NI vs ZIKV are underscored in **bold** format. Differences between ZIKV females vs
 211 ZIKV males are highlighted by **bold-underlined** format. No significant differences were observed
 212 between NI females vs NI males. Score represents the fold change (analyte median value in infected
 213 patient divided by analyte median value in controls) segregated by gender.

214

215 **Bimodal viremia is accompanied by increased levels of a defined group of** 216 **biomarkers**

217 Viremia and biomarkers were assessed at different time-points (Day 1 post-infection
 218 denoted as D1 etc.) D1 (n=11); D2 (n=13); D3 (n=10); D4 (n=09) and D5 (n=05). A
 219 bimodal distribution was observed, with two viremia peaks at D2 and D4, reaching the
 220 lowest levels at D5 (Fig 3, gray panel). Dynamics of CCL5, TNF- α , IFN- γ , IL-17 and
 221 G-CSF were closely related to viremia (Fig 3A). A similar bimodal distribution was
 222 observed for IL-1 β and IL-13 (Fig 3B). The highest levels of CXCL8 and CCL2 were
 223 observed at D1 and D2 (Fig 3C). An inverse correlation was observed for IL-12, IL-10
 224 and VEGF (Fig 3D), where the highest levels coincide with the lowest viremias. The
 225 levels of CCL3, CXCL10, IL-6 and FGF-basic display a distinct pattern, with the lowest
 226 levels observed at D3, coinciding with the first drop of viremia (Fig 3E). A valley at D4

227 followed by an increase at D5 was observed for CCL11, CCL4, IL-1Ra, and IL-4 (Fig
228 3F), and unique patterns were observed for IL-5, IL-9, PDGF, and GM-CSF (Fig 3G).

229

230 **Fig 3. Rhythms of Viremia, Chemokines, Cytokines and Growth Factors Early**
231 **After Zika Virus Infection in Adults.** Cross-sectional follow-up of viremia and serum
232 biomarkers was carried out in Zika virus-infected patients categorized according to the
233 time (days) upon symptoms onset (D1, n=11; D2, n=13; D3, n=10; D4 n=09 and D5
234 n=05). Viremia ($1/CT \times 100$) displayed a bimodal profile with similar waves at D2 and
235 D4 (gray panel). Distinct patterns were identified for clusters of biomarkers as they
236 displayed kinetic curves shaping a bimodal wave at D2 and higher wave [\uparrow] at D4
237 (panel A, for CCL5, TNF- α , IFN- γ , IL-17 and G-CSF); a bimodal profile with similar
238 waves at D2 and D4 (panel B, IL-1 β and IL-13); a wave at D2 and a valley at D3 (panel
239 C, CXCL8 and CCL2); a midpoint wave at D3 (panel D, IL-12, IL-10 and VEGF); an
240 unimodal valley at D3 (panel E, CCL3, CXCL10, IL-6 and FGF-basic); a valley at D4
241 (panel F, CCL11, CCL4, IL-1Ra and IL-4) or an unique pattern (panel G, IL-5, IL-9,
242 PDGF and GM-CSF). Data are displayed as global maximum equalized median values
243 of the serum concentrations (pg/mL) for each biomarker.

244

245 Biomarkers were also evaluated in controls, and the IQR are represented by dashed lines
246 (Fig 4). Most of biomarkers' levels differ between patients and controls at all time-
247 points, except for IL-10 at D1 and D2, IL-1 β at D3. No differences were observed for
248 IL-9.

249

250 **Fig 4. Kinetics of Viremia, Serum Chemokines, Cytokines and Growth Factors**
251 **Early After Zika Virus Infection in Adults.** Cross-sectional analysis of viremia and

252 serum biomarkers was performed in Zika virus-infected patients categorized according
253 to the time (days) upon symptoms onset (D1, n=11; D2, n=13; D3, n=10; D4 n=09 and
254 D5 n=05). Data expressed as pg/mL are displayed in box and whiskers (10-90
255 percentile) plots. Multiple comparisons amongst distinct time-points upon symptoms
256 onset were performed by Kruskal-Wallis followed by Dunn's post-test and significant
257 differences at $p < 0.05$ underscored by D1, D2, D3 and D4 as they correspond to specific
258 time-points. Comparative analysis with non-infected controls (NI) was also carried out
259 at each time-point by Mann-Whitney test and significant differences at $p < 0.05$
260 underscored by asterisks (*). Reference ranges for each biomarker were established as
261 interquartile ranges (25th-75th percentiles) observed in NI (dashed lines). Distinct
262 patterns were identified for clusters of biomarkers as they displayed kinetic curves
263 shaping a bimodal wave at D2 and higher wave [↑] at D4 (CCL-5, TNF- α , IFN- γ , IL-17
264 and G-CSF); a bimodal profile with similar waves at D2 and D4 (IL-1 β and IL-13); a
265 wave at D2 and a valley at D3 (CXCL8 and CCL2); a midpoint wave at D3 (IL-12, IL-
266 10 and VEGF); an unimodal valley at D3 (CCL3, CXCL10, IL-6 and FGF-basic); a
267 valley at D4 (CCL11, CCL4, IL-1Ra and IL-4) or an unique pattern (IL-5, IL-9, PDGF
268 and GM-CSF).

269

270 **ZIKV infection elicited a set of general and timeline-specific biomarkers**

271 The biomarker levels were used to build a signature (Fig 5, left panels) as described in
272 the methods section. A significant difference in the overall profile was observed in
273 ZIKV-infected cases (Fig 5, top-left panel). Furthermore, the radar chart revealed that
274 19/24 (79%) biomarkers were highly induced by ZIKV infection (Fig 5, bottom-left
275 panel). Almost all biomarkers analyzed were found in levels above the global median in
276 more than 75% of the infected patients.

277 Venn diagram analysis showed that four chemokines (CCL4, CCL2, CCL5, CXCL10);
278 two cytokines (IL-6, IL-4) and two growth factors (PDGF, G-CSF) were significantly
279 induced in all time-points (Fig 5, right panel). Of note, TNF- α appears as a single
280 biomarker at the intersection of the viremia peaks (D2 and D4). In contrast, IL-10 is the
281 only unregulated biomarker at viremia valleys (D3 and D5) while increased levels of
282 IL-12 appears at D5 (Fig 5, inserted table).

283

284 **Fig 5. General and Timeline Biomarkers upon Symptoms Onset Early After Zika**
285 **Virus Infection in Adults.** Biomarker signatures of NI (\square) and ZIKV (\blacksquare) were
286 constructed as described in methods. Data are presented in radar charts as the proportion
287 of subjects with serum biomarker levels above the global population median values (NI
288 plus ZIKV). Biomarkers with levels above the global median in more than 75% of
289 subjects were highlighted by asterisks (*). The Venn diagram shows the intersections
290 with common attributes as well as selective biomarkers along the timeline of symptoms
291 onset (Day 1; Day 2; Day 3; Day 4 and Day 5). Venn diagram report summarizes
292 selected attributes with patterns labeled as (a) universal; (b) peak of viremia; (c) valley
293 of viremia or (d) late biomarkers (inserted table).

294

295 **Distinct biomarker networks are observed at different time-points**

296 Cytoscape software was used to assemble correlative analysis of immunological
297 biomarkers. The exploratory analysis demonstrated that earlier infection was associated
298 with more imbricate and complex biomarker networks. Most correlations at D1 and all
299 correlations at D2 were positive (solid lines). The level of complexity decreased from
300 D1 to D5. However, the interactions were more complex at D2 and D4, concomitant
301 with the viremia peaks (Fig 6).

302

303 **Fig 6. Timeline Biomarker Networks Early After Zika Virus Infection in Adults.**

304 Systems integrative biology analysis of attributes was assembled using Cytoscape
305 software platform to build circular nodal network layout for each time-point upon Zika
306 virus infection day 1 (D1) up day 5 (D5) based on Spearman's correlation matrices.
307 Significance was considered at $p < 0.05$. The timeline of networks is displayed as circular
308 layouts to characterize the interaction along the early time-points. Colored nodes were
309 employed to identify chemokines (CH), pro-inflammatory cytokines (PI), regulatory
310 cytokines (RG) and growth factors (GF). Connecting edges were drawn to underscore
311 the association between attributes, classified as positive (solid line) or negative (dashed
312 line).

313

314 **High-dimensional data analysis elected CXCL10 as the most promising biomarker**
315 **for a putative clinical application**

316 A heatmap matrix was constructed to evaluate the profile of biomarkers associated with
317 ZIKV infection. This analysis demonstrated that CXCL10 clustered most patients,
318 segregating them from controls. Additionally, a decision tree was built to identify the
319 biomarker most able to segregate patients. This approach confirmed the heatmap
320 observations indicating CXCL10 as the most relevant element, followed by IL-4 and
321 VEGF. The analysis showed a very high global accuracy (99.4%) with a leave-one-out-
322 cross-validation of 96.8% (Fig 7). The significance of these attributes (CXCL10, IL-4
323 and VEGF) was assessed by 3D-plots and the performance of the root attribute
324 (CXCL10) evaluated by scatter plot distribution and ROC curve analysis (Fig 7, bottom
325 panels). CXCL10 alone lead to a very high global accuracy ranging from 0.952-0.998.
326 Together, the results demonstrated that CXCL10 measurement ascertains 94% of the

327 patients, with no false-positive identification and outstanding indices (co-positivity, co-
328 negativity and likelihood ratio).

329

330 **Fig 7. High-dimensional Data Analysis Early After Zika Virus Infection in Adults.**

331 Machine-learning high-dimensional data approaches were applied to further explore and
332 identify feasible criteria applicable for the clinical follow-up of Zika virus infection. (A)
333 Heatmap panels were built to verify the ability of attributes to segregate ZIKV (■) and
334 NI (■) groups as they present low (■) or high (■) levels of serum biomarkers. Decision
335 tree algorithms were generated define root and branch attributes to segregate patients
336 (ZIKV=■) from non-infected controls (NI=■). Global accuracy and leave-one-out-
337 cross-validation (LOOCV) values are provided in the figure. The root/branch attributes
338 selected by the decision tree algorithm were compiled into a 3D-plot to verify their
339 clusterization strength. The performance of the selected root attribute to discriminate
340 ZIKV (●) from NI (●) was evaluated by scatter plot distribution and validated by
341 receiver operating-characteristic indices (Area under the curve, AUC; Co-positivity, Cp;
342 Co-negativity, Cn; Positive/Negative Likelihood Ratio, LR+/LR-).

343

344 **Discussion**

345 The pathogenesis of ZIKV infection is still largely unknown, and the main determinants
346 of disease manifestations are not yet well established. Understanding serum
347 immunomodulators during acute infection may be a first step to elucidate the
348 mechanisms underlying ZIKV-induced immunopathology.

349 We show that the immune response during the acute phase of ZIKV infection is
350 polyfunctional and broadly inflammatory as evidenced by significant elevated levels of
351 IL-4, IL-17, IFN- γ , IL-1 β , IL-1Ra, TNF- α and IL-6 in patients. This is consistent with

352 findings from Kam et al [9] that also found a robust pro-inflammatory cytokine response
353 during acute ZIKV infection with elevations of IL-18, TNF- α , IFN- γ , IL-8, IL-6, GRO- α ,
354 and IL-7. Alternatively, when we stratified the results by gender, ZIKV-infected males
355 presented lower levels of CCL3, CCL4, CCL5, IL-17, FGF-basic and GM-CSF. The
356 reason for this difference is unknown in the context of ZIKV infection, however this
357 finding is consistent with the literature demonstrating that females tend to mount a
358 higher innate and adaptive immune system response to viruses compared to men [14].
359 In addition, this result may also be explained as females were sampled on average one
360 day earlier than men with the median time from onset to diagnostic sampling (Females=
361 day 2; Males= day 3).

362 It is possible that previous exposure to Flavivirus antigens may affect the immune
363 response to ZIKV infection. In the present study, almost all patients (51/54) exhibited
364 positive DENV IgG antibodies. Manaus has had several dengue epidemics, including
365 co-circulation of different serotypes [15-17]. Moreover, the Amazonas State is endemic
366 for Yellow Fever virus (YFV) and has a very high YFV-vaccination coverage. Thus,
367 mostly individuals enrolled in this study have experienced previous Flavivirus exposure
368 potentially modulating the cytokine and chemokine responses. These differences in
369 prior Flavivirus exposure may account for some differences in cytokine and chemokine
370 profiles shown by Kam et al. that examined a Brazilian cohort of patients from
371 Campinas, Brazil where Yellow Fever vaccination was not required by the government
372 at the time of their study as it is in Manaus, Brazil.

373 Similar to our results, comparable immune response induced during the acute phase has
374 previously been described in infections caused by ZIKV and other Flaviviruses,
375 including YFV, DENV and West Nile virus [8,18-20]. In the case of ZIKV infection,
376 the mechanism of inflammatory immune response is not clearly delineated. The

377 immune response may be triggered by viral upregulation of expression of pattern
378 recognition receptors (PRRs) engaged in downstream pathways and inflammatory
379 antiviral response such as IRF7, IFN- α , IFN- β , and CCL5 [7]. Interestingly, we showed
380 a strong positive correlation between IFN- α and CCL5, suggesting that the synergistic
381 effect of these cytokines might be crucial on the outcomes of the acute inflammation
382 caused by ZIKV.

383 Our findings also revealed higher levels of growth factors and chemokines among
384 patients. Likewise, increased levels of CXCL10, CCL5, CCL3 and VEGF were
385 primarily demonstrated in patients acutely infected with ZIKV, while elevated levels of
386 GM-CSF, CCL4, and FGF-basic biomarkers only in the recovery phase [8]. Our study
387 demonstrated that all chemokines and growth factors analyzed were significantly
388 increased in the acute phase in comparison with non-infected controls. In fact, the role
389 of growth factors in the pathogenesis of arboviruses infections remains a matter of
390 debate [20-22]. We demonstrate that a remarkable increase of FGF-basic, PDGF,
391 VEGF, G-CSF and GM-CSF identifies the acute phase of ZIKV infection, which
392 suggests the importance of chemokines and growth factors in the initiation and
393 regulation of the acute-phase immune response.

394 Similarly, increased serum concentrations of both CXCL (CXCL8 and CXCL10) and
395 CCL chemokines (CCL2, CCL3, CCL4, CCL5, and CCL11) were found in acute ZIKV
396 infection. The role of CCL5 in the arbovirus-induced immunopathology remains a
397 controversial issue, but this chemokine along with CCL2 and CCL3 were previously
398 linked to severity of dengue and Japanese encephalitis virus infections, including
399 neurological diseases and impairment of neuronal survival [23-27].

400 Furthermore, we found strong correlations between TNF- α and CCL5 concentrations
401 and percentages of circulating neutrophils and lymphocytes in acute ZIKV infection.

402 This finding is likely due to the role of TNF- α and CCL5 in leukocyte chemo attraction
403 [28,29] and demonstrates the important role of this cytokine and chemokine in
404 stimulation of the innate and adaptive immune system in response to ZIKV infection.
405 In addition, this manuscript is the first to describe the bimodal nature of viremia in acute
406 Zika infection and corresponding peaks in inflammatory cytokine production. A
407 biological model explaining bimodal viremia was firstly described in the classical study
408 of Fenner's with the Mousepox virus [30]. Similarly, Flaviviruses are initially replicated
409 in Langerhans cells at the site of inoculation and in draining regional
410 lymph nodes. Despite a robust anti-viral innate immune response that eliminates viral
411 infected cells, some virus particles are disseminated by blood (primary viremia).
412 Therefore, several organs and tissues may become infected producing a second wave
413 of viral replication that reaches blood causing a secondary viremia [31]. The equine
414 infection by African Horse Sickness Viruses, another arbovirus of the *Orbivirus* genus,
415 *Reoviridae* family, also shows two viremia peaks. The first peak is observed after the
416 viral multiplication into lymph nodes, whereas the second peak is observed after viral
417 replication in spleen, lungs and endothelial cells [32]. Several arboviruses are known
418 to cause prolonged viremia into their natural hosts, and this is well documented for
419 encephalitic Alphaviruses [33,34] leading to higher transmission rates for mosquito
420 vectors. Interestingly, bimodal viremia has been found in patients after low dose live
421 attenuated 17DD Yellow Fever vaccine administration [35]. The low dose live
422 attenuated vaccine is hypothesized to elicit a less robust immune response in
423 comparison to the standard dosage vaccine that does not clear the initial viremia leading
424 to a second peak of viremia a few days later. Further research to determine if ZIKV
425 undergoes similar processes is needed.

426 In this manuscript, we reported high levels of pro-inflammatory mediators during
427 the acute phase of ZIKV infection. Paradoxically, although the inflammatory response
428 leads to viral clearance, the high levels of circulating pro-inflammatory biomarkers may
429 facilitate the transmission of viruses from circulation to the central nervous system by
430 increasing the permeability of the blood brain barrier. This phenomenon has been
431 already reported for the West Nile virus [36], another neurovirulent Flavivirus, and may
432 partially explain ZIKV neuroinvasiveness.

433 Remarkably, the CXCL10 was expressed greater than 200-fold in ZIKV-infected
434 subjects. Augmented serum levels of CXCL10 have been found during severe clinical
435 manifestations of dengue and Yellow fever [14,18,37]. CXCL10 has also been shown to
436 play an important role in CD-8+ T-cell recruitment as part of an anti-flaviviral response
437 in the central nervous system to West Nile virus [38] and dengue virus [39].

438 Furthermore, CXCL10 has been previously associated as a biomarker of severity in
439 several diseases including those caused by bacteria like *Mycobacterium tuberculosis*
440 and *Legionella pneumophila*; protozoans like *Trypanosoma brucei*, *Leishmania major*,
441 *Plasmodium vivax* or *Plasmodium falciparum* [40]; viral diseases such as in Simian
442 Human Immunodeficiency Virus Encephalitis [41] and viral acute respiratory infection
443 in healthy adults, mainly those caused by Influenza virus [42].

444 Of paramount importance, CXCL10 overexpression has been observed in non-
445 infectious neuronal diseases like Alzheimer's and multiple sclerosis, and in infectious
446 diseases like HIV-associated dementia [43]. Furthermore, different studies showed that
447 the over-expression of CXCL10 leads to apoptosis in fetal neurons [40] that is triggered
448 by intracellular Ca(2+) elevation activating caspase-9 and caspase-3 [43]. CXCL10 has
449 also been strongly implicated in Guillain-Barré syndrome pathogenesis [44]. Thus, we
450 hypothesize that the high elevations of CXCL10 in ZIKV patients may contribute to

451 neuronal damage affecting the developing fetal brain and potentially targeting
452 peripheral nerves in Guillain-Barré syndrome as well. Consistent with this hypothesis,
453 Kam et al. specifically identified higher levels of CXCL10 in ZIKV-infected patients with
454 neurological complications compared to those without and higher levels of CXCL10 in
455 ZIKV-infected pregnant women carrying babies with fetal growth associated
456 malformations.
457 High levels of CXCL10 have been previously described at acute and convalescent
458 phases, with more prominent expression at the latter [8]. Unfortunately, although our
459 data strongly suggest CXCL10 as a biomarker of ZIKV acute infection, we were unable
460 to perform a longitudinal analysis to verify its kinetics across different stages of the
461 disease, to further confirm whether the concentrations of this chemokine would be down
462 or up-regulated. In addition, CXCL10 elevation is also observed in pre-eclampsia and
463 hypertension found in pregnancy resulting in a range of fetal injuries, including
464 intrauterine growth retardation and neurological damage induced by hypoxia [45,46].
465 Thus, it is reasonable to suggest that ZIKV-induced inflammation may increase fetal
466 injuries.
467 CXCL10 may also be an important therapeutic target [40]. For example, CXCL10
468 neutralization by specific antibodies or genetic deletion in CXCL10^{-/-} mice protected
469 against cerebral malaria infection and inflammation [47]. Passive transfer of anti-
470 CXCL10 antibodies reduced inflammatory leukocyte recruitment across the blood brain
471 barrier. Furthermore, statin medications commonly used for cholesterol control have
472 been shown to decrease CXCL10 and to be effective in CXCL10 mediated Crohn's
473 disease [48].
474 Finally, we describe the relationship between the timing of viremia and cytokine
475 elevations. The acute phase of ZIKV infection lasts around five days [49]. This study

476 assessed the acute phase biomarkers and viral titers at different time-points (until day 5).
477 Augmented levels of CCL4, CCL2, CCL5, CXCL5, CXCL10, IL-6, IL-4, PDGF, and
478 G-CSF immunomodulators were observed at all time-points. The peak of viremia, at
479 Day 2 and Day 4, was accompanied by increased TNF- α levels. Instead, the IL-10
480 elevation appeared to be directly related to the lowest virus titers (Day 3 and Day 5),
481 while the highest levels of IL-12 were found at Day 5. These findings allow us to
482 deduce that the acute phase of ZIKV is characterized mainly by an innate immune
483 system inflammatory response, with the overlap of the inflammatory biomarkers and
484 viremia peaks, and anti-inflammatory response coinciding with viremia decay.

485 Altogether, this study identifies unique characteristics of the acute inflammatory and
486 multifactorial immune response induced by ZIKV and depicts CXCL10 as a potential
487 biomarker of the acute infection, perhaps, a predictor of severity. Nevertheless, further
488 longitudinal studies that measure the host immunopathological aspects at several time-
489 points is required to better characterize all the immunological factors involved in the
490 Zika disease. The elevated concentrations of serum biomarkers observed in this study,
491 may bring new insights to the ZIKV immunopathology puzzle.

492

493 **Acknowledgments**

494 The authors are thankful to the Programa de Desenvolvimento Tecnológico em Insumos
495 para a Saúde - PDTIS-FIOCRUZ for the use the flow cytometry (CPqRR) and Real-
496 Time PCR (ILMD) facilities.

497

498 **References**

499 1. Musso D, Gubler DJ. Zika Virus. Clin Microbiol Rev. American Society for
500 Microbiology; 2016;29: 487–524. doi:10.1128/CMR.00072-15

- 501 2. Duffy MR, Chen T-H, Hancock WT, Powers AM, Kool JL, Lanciotti RS, et al.
502 Zika virus outbreak on Yap Island, Federated States of Micronesia. *N Engl J*
503 *Med.* 2009;360: 2536–2543. doi:10.1056/NEJMoa0805715
- 504 3. Oehler E, Watrin L, Larre P, Leparc-Goffart I, Lastere S, Valour F, et al. Zika
505 virus infection complicated by Guillain-Barre syndrome--case report, French
506 Polynesia, December 2013. *Euro Surveill.* 2014;19.
- 507 4. Kleber de Oliveira W, Cortez-Escalante J, De Oliveira WTGH, do Carmo GMI,
508 Henriques CMP, Coelho GE, et al. Increase in Reported Prevalence of
509 Microcephaly in Infants Born to Women Living in Areas with Confirmed Zika
510 Virus Transmission During the First Trimester of Pregnancy - Brazil, 2015.
511 *MMWR Morb Mortal Wkly Rep.* 2016;65: 242–247.
512 doi:10.15585/mmwr.mm6509e2
- 513 5. Cauchemez S, Besnard M, Bompard P, Dub T, Guillemette-Artur P, Eyrolle-
514 Guignot D, et al. Association between Zika virus and microcephaly in French
515 Polynesia, 2013–15: a retrospective study. *The Lancet.* Elsevier; 2016;387:
516 2125–2132. doi:10.1016/S0140-6736(16)00651-6
- 517 6. França GVA, Schuler-Faccini L, Oliveira WK, Henriques CMP, Carmo EH, Pedi
518 VD, et al. Congenital Zika virus syndrome in Brazil: a case series of the first
519 1501 livebirths with complete investigation. *Lancet.* Elsevier; 2016;388: 891–
520 897. doi:10.1016/S0140-6736(16)30902-3
- 521 7. Hamel R, Dejarnac O, Wichit S, Ekchariyawat P, Neyret A, Luplertlop N, et al.
522 Biology of Zika Virus Infection in Human Skin Cells. Diamond MS, editor. *J*
523 *Virol.* American Society for Microbiology; 2015;89: 8880–8896.
524 doi:10.1128/JVI.00354-15
- 525 8. Tappe D, Pérez-Girón JV, Zammarchi L, Rissland J, Ferreira DF, Jaenisch T, et
526 al. Cytokine kinetics of Zika virus-infected patients from acute to reconvalescent
527 phase. *Med Microbiol Immunol.* Springer Berlin Heidelberg; 2015;205: 1–5.
528 doi:10.1007/s00430-015-0445-7
- 529 9. Kam YW, Leite JA, Lum FM, Tan J. Specific biomarkers associated with
530 neurological complications and congenital CNS abnormalities from Zika virus-
531 infected patients in Brazil. *The Journal of* 2017.
- 532 10. Lanciotti RS, Kosoy OL, Laven JJ, Velez JO, Lambert AJ, Johnson AJ, et al.
533 Genetic and Serologic Properties of Zika Virus Associated with an Epidemic,
534 Yap State, Micronesia, 2007. *Emerging Infect Dis.* Centers for Disease Control
535 and Prevention; 2008;14: 1232–1239. doi:10.3201/eid1408.080287
- 536 11. Lanciotti RS, Kosoy OL, Laven JJ, Panella AJ, Velez JO, Lambert AJ, et al.
537 Chikungunya virus in US travelers returning from India, 2006. *Emerging Infect*
538 *Dis.* 2007;13: 764–767. doi:10.3201/eid1305.070015
- 539 12. Gurukumar KR, Priyadarshini D, Patil JA, Bhagat A, Singh A, Shah PS, et al.
540 Development of real time PCR for detection and quantitation of Dengue Viruses.
541 *Virol J.* BioMed Central Ltd; 2009;6: 10. doi:10.1186/1743-422X-6-10

- 542 13. Luiza-Silva M, Campi-Azevedo AC, Batista MA, Martins MA, Avelar RS, da
543 Silveira Lemos D, et al. Cytokine signatures of innate and adaptive immunity in
544 17DD yellow fever vaccinated children and its association with the level of
545 neutralizing antibody. *J Infect Dis.* Oxford University Press; 2011;204: 873–883.
546 doi:10.1093/infdis/jir439
- 547 14. Klein SL. Sex influences immune responses to viruses, and efficacy of
548 prophylaxis and treatments for viral diseases. *Bioessays.* WILEY-VCH Verlag;
549 2012;34: 1050–1059. doi:10.1002/bies.201200099
- 550 15. De Figueiredo RMP, Thatcher BD, de Lima ML, Almeida TC, Alecrim WD,
551 Guerra MV de F. [Exanthematous diseases and the first epidemic of dengue to
552 occur in Manaus, Amazonas State, Brazil, during 1998-1999]. *Rev Soc Bras Med*
553 *Trop.* 2004;37: 476–479.
- 554 16. Figueiredo RMP de, Naveca FG, Oliveira CM, Bastos M de S, Mourão MPG,
555 Viana S de S, et al. Co-infection of Dengue virus by serotypes 3 and 4 in patients
556 from Amazonas, Brazil. *Rev Inst Med Trop Sao Paulo.* 2011;53: 321–323.
- 557 17. Figueiredo RMP de, Naveca FG, Bastos M de S, Melo MDN, Viana S de S,
558 Mourão MPG, et al. Dengue virus type 4, Manaus, Brazil. *Emerging Infect Dis.*
559 2008;14: 667–669. doi:10.3201/eid1404.071185
- 560 18. de-Oliveira-Pinto LM, Marinho CF, Povia TF, de Azeredo EL, de Souza LA,
561 Barbosa LDR, et al. Regulation of inflammatory chemokine receptors on blood T
562 cells associated to the circulating versus liver chemokines in dengue fever. Proost
563 P, editor. *PLoS ONE.* Public Library of Science; 2012;7: e38527.
564 doi:10.1371/journal.pone.0038527
- 565 19. Meulen ter J, Sakho M, Koulemou K, Magassouba N, Bah A, Preiser W, et al.
566 Activation of the cytokine network and unfavorable outcome in patients with
567 yellow fever. *J Infect Dis.* Oxford University Press; 2004;190: 1821–1827.
568 doi:10.1086/425016
- 569 20. Kumar M, Verma S, Nerurkar VR. Pro-inflammatory cytokines derived from
570 West Nile virus (WNV)-infected SK-N-SH cells mediate neuroinflammatory
571 markers and neuronal death. *J Neuroinflammation.* BioMed Central; 2010;7: 73.
572 doi:10.1186/1742-2094-7-73
- 573 21. Rothman AL. Immunity to dengue virus: a tale of original antigenic sin and
574 tropical cytokine storms. *Nat Rev Immunol.* 2011;11: 532–543.
575 doi:10.1038/nri3014
- 576 22. Tseng C-S, Lo H-W, Teng H-C, Lo W-C, Ker C-G. Elevated levels of plasma
577 VEGF in patients with dengue hemorrhagic fever. *FEMS Immunol Med*
578 *Microbiol.* The Oxford University Press; 2005;43: 99–102.
579 doi:10.1016/j.femsim.2004.10.004
- 580 23. Chirathaworn C, Poovorawan Y, Lertmaharit S, Wuttirattanakowit N. Cytokine
581 levels in patients with chikungunya virus infection. *Asian Pac J Trop Med.*
582 2013;6: 631–634. doi:10.1016/S1995-7645(13)60108-X

- 583 24. Sathupan P, Khongphattanayothin A, Srisai J, Srikaew K, Poovorawan Y. The
584 role of vascular endothelial growth factor leading to vascular leakage in children
585 with dengue virus infection. *Ann Trop Paediatr.* 2007;27: 179–184.
586 doi:10.1179/146532807X220280
- 587 25. Werner S, Grose R. Regulation of wound healing by growth factors and
588 cytokines. *Physiol Rev. American Physiological Society;* 2003;83: 835–870.
589 doi:10.1152/physrev.00031.2002
- 590 26. Hiley CT, Chard LS, Gangeswaran R, Tysome JR, Briat A, Lemoine NR, et al.
591 Vascular endothelial growth factor A promotes vaccinia virus entry into host
592 cells via activation of the Akt pathway. *J Virol. American Society for*
593 *Microbiology;* 2013;87: 2781–2790. doi:10.1128/JVI.00854-12
- 594 27. Zlotnik A, Yoshie O. The chemokine superfamily revisited. *Immunity. Elsevier;*
595 *2012;36: 705–716.* doi:10.1016/j.immuni.2012.05.008
- 596 28. Ming WJ, Bersani L, Mantovani A. Tumor necrosis factor is chemotactic for
597 monocytes and polymorphonuclear leukocytes. *J Immunol.* 1987;138: 1469–
598 1474.
- 599 29. Murooka TT, Rahbar R, Plataniias LC, Fish EN. CCL5-mediated T-cell
600 chemotaxis involves the initiation of mRNA translation through mTOR/4E-BP1.
601 *Blood. American Society of Hematology;* 2008;111: 4892–4901.
602 doi:10.1182/blood-2007-11-125039
- 603 30. FENNER F. The pathogenesis of the acute exanthems; an interpretation based on
604 experimental investigations with mousepox; infectious ectromelia of mice. *The*
605 *Lancet.* 1948;2: 915–920.
- 606 31. Murray PR, Rosenthal KS, Pfaller MA. *Medical Microbiology. Elsevier Health*
607 *Sciences;* 2015.
- 608 32. Mellor PS, Hamblin C. African horse sickness. *Vet Res. EDP Sciences;* 2004;35:
609 445–466. doi:10.1051/vetres:2004021
- 610 33. Bowen GS. Prolonged western equine encephalitis viremia in the Texas tortoise
611 (*Gopherus berlandieri*). *Am J Trop Med Hyg.* 1977;26: 171–175.
- 612 34. Paessler S, Pfeffer M. Togaviruses Causing Encephalitis. *Encyclopedia of*
613 *Virology. Elsevier;* 2008. pp. 76–82. doi:10.1016/B978-012374410-4.00630-0
- 614 35. Campi-Azevedo AC, de Almeida Estevam P, Coelho-Dos-Reis JG, Peruhype-
615 Magalhães V, Villela-Rezende G, Quaresma PF, et al. Subdoses of 17DD yellow
616 fever vaccine elicit equivalent virological/immunological kinetics timeline. *BMC*
617 *Infect Dis. BioMed Central;* 2014;14: 391. doi:10.1186/1471-2334-14-391
- 618 36. Wang T, Town T, Alexopoulou L, Anderson JF, Fikrig E, Flavell RA. Toll-like
619 receptor 3 mediates West Nile virus entry into the brain causing lethal
620 encephalitis. *Nat Med.* 2004;10: 1366–1373. doi:10.1038/nm1140
- 621 37. Melchjorsen J, Sørensen LN, Paludan SR. Expression and function of

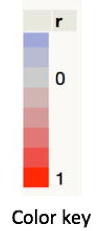
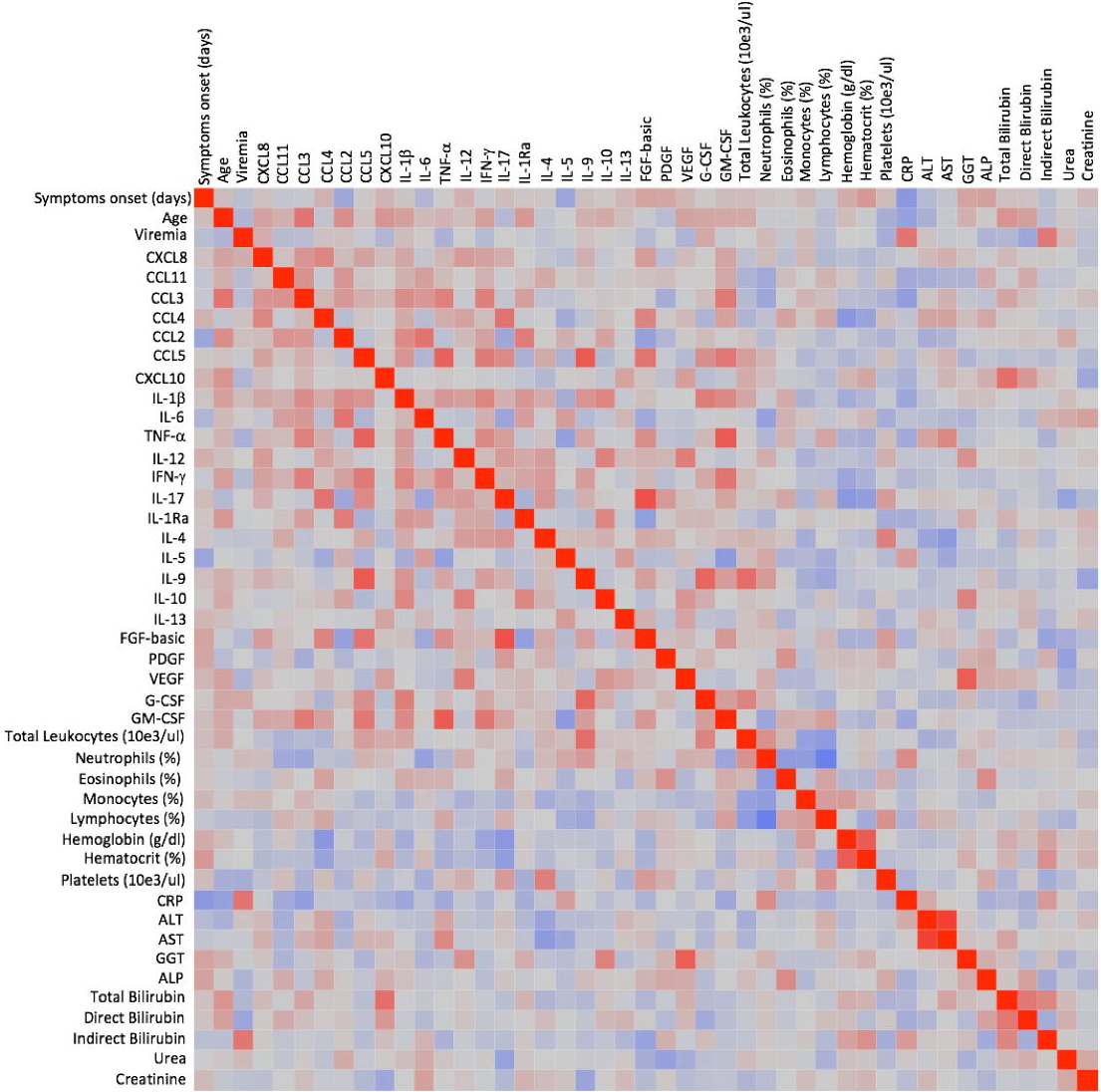
- 622 chemokines during viral infections: from molecular mechanisms to in vivo
623 function. *J Leukoc Biol.* 2003;74: 331–343.
- 624 38. Klein RS, Lin E, Zhang B, Luster AD, Tollett J, Samuel MA, et al. Neuronal
625 CXCL10 directs CD8+ T-cell recruitment and control of West Nile virus
626 encephalitis. *J Virol. American Society for Microbiology*; 2005;79: 11457–
627 11466. doi:10.1128/JVI.79.17.11457-11466.2005
- 628 39. Hsieh M-F, Lai S-L, Chen J-P, Sung J-M, Lin Y-L, Wu-Hsieh BA, et al. Both
629 CXCR3 and CXCL10/IFN-inducible protein 10 are required for resistance to
630 primary infection by dengue virus. *J Immunol.* 2006;177: 1855–1863.
- 631 40. Liu M, Guo S, Hibbert JM, Jain V, Singh N, Wilson NO, et al. CXCL10/IP-10 in
632 infectious diseases pathogenesis and potential therapeutic implications. *Cytokine*
633 *Growth Factor Rev.* 2011;22: 121–130. doi:10.1016/j.cytogfr.2011.06.001
- 634 41. Sui Y, Potula R, Dhillon N, Pinson D, Li S, Nath A, et al. Neuronal apoptosis is
635 mediated by CXCL10 overexpression in simian human immunodeficiency virus
636 encephalitis. *Am J Pathol.* 2004;164: 1557–1566. doi:10.1016/S0002-
637 9440(10)63714-5
- 638 42. Hayney MS, Henriquez KM, Barnet JH, Ewers T, Champion HM, Flannery S, et
639 al. Serum IFN- γ -induced protein 10 (IP-10) as a biomarker for severity of acute
640 respiratory infection in healthy adults. *J Clin Virol.* 2017;90: 32–37.
641 doi:10.1016/j.jcv.2017.03.003
- 642 43. Sui Y, Stehno-Bittel L, Li S, Loganathan R, Dhillon NK, Pinson D, et al.
643 CXCL10-induced cell death in neurons: role of calcium dysregulation. *Eur J*
644 *Neurosci.* Blackwell Publishing Ltd; 2006;23: 957–964. doi:10.1111/j.1460-
645 9568.2006.04631.x
- 646 44. Chiang S, Ubogu EE. The role of chemokines in Guillain-Barré syndrome.
647 *Muscle Nerve.* 2013;48: 320–330. doi:10.1002/mus.23829
- 648 45. Gotsch F, Romero R, Friel L, Kusanovic JP, Espinoza J, Erez O, et al.
649 CXCL10/IP-10: a missing link between inflammation and anti-angiogenesis in
650 preeclampsia? *J Matern Fetal Neonatal Med.* 2007;20: 777–792.
651 doi:10.1080/14767050701483298
- 652 46. Uzan J, Carbonnel M, Piconne O, Asmar R, Ayoubi J-M. Pre-eclampsia:
653 pathophysiology, diagnosis, and management. *Vasc Health Risk Manag.* Dove
654 Press; 2011;7: 467–474. doi:10.2147/VHRM.S20181
- 655 47. Nie CQ, Bernard NJ, Norman MU, Amante FH, Lundie RJ, Crabb BS, et al. IP-
656 10-mediated T cell homing promotes cerebral inflammation over splenic
657 immunity to malaria infection. Riley EM, editor. *PLoS Pathog.* Public Library of
658 Science; 2009;5: e1000369. doi:10.1371/journal.ppat.1000369
- 659 48. Grip O, Janciauskiene S. Atorvastatin reduces plasma levels of chemokine
660 (CXCL10) in patients with Crohn's disease. Timmer A, editor. *PLoS ONE.*
661 Public Library of Science; 2009;4: e5263. doi:10.1371/journal.pone.0005263

- 662 49. Nayak S, Lei J, Pekosz A, Klein S, Burd I. Pathogenesis and Molecular
663 Mechanisms of Zika Virus. *Semin Reprod Med.* Thieme Medical Publishers;
664 2016;34: 266–272. doi:10.1055/s-0036-1592071

665

Fig 1. Immunological biomarkers correlations with the results of routine laboratorial tests, age, viremia, and symptoms

Correlation Matrix



Correlation Indices

Source attributes	Target attributes	Spearman ρ	p values
ALP	Viremia	-0,5613	0,01
ALT	CCL4	0,4492	0,04
AST	IL-4	-0,5532	0,01
AST	CXCL10	0,457	0,04
AST	CCL4	0,4764	0,03
AST	CCL5	0,4554	0,04
C-reactive protein (CRP)	Symptoms onset (days)	-0,4886	0,03
C-reactive protein (CRP)	Viremia	0,5449	0,01
C-reactive protein (CRP)	CXCL10	-0,4976	0,03
C-reactive protein (CRP)	CCL3	-0,4645	0,04
Creatinine	IL-9	-0,6443	0,001
Direct Bilirubin	G-CSF	-0,5576	0,01
GGT	IL-10	0,4671	0,04
GGT	VEGF	0,5969	0,007
Hematocrit (%)	IL-17	-0,5144	0,01
Hematocrit (%)	CCL4	-0,4756	0,02
Hemoglobin (g/dL)	IL-1β	-0,437	0,04
Hemoglobin (g/dL)	IL-9	-0,4476	0,04
Hemoglobin (g/dL)	IL-17	-0,6159	0,003
Hemoglobin (g/dL)	IFN-γ	-0,4946	0,02
Hemoglobin (g/dL)	CCL4	-0,4678	0,03
Indirect Bilirubin	FGF basic	-0,4542	0,04
Lymphocytes (%)	CCL8	-0,4811	0,03
Monocytes (%)	IL-9	-0,4497	0,04
Neutrophils (%)	IL-13	0,509	0,02
Platelets (10 ³ /μL)	Viremia	-0,4333	0,04
Total Leukocytes (10 ³ /μL)	IL-9	0,6071	0,003
Total Leukocytes (10 ³ /μL)	IL-10	0,4709	0,03
Urea	IL-17	-0,4564	0,04
Urea	PDGF-bb	-0,4928	0,02

Fig 2. Panoramic Overview of Serum Chemokines, Cytokines and Growth Factors Early After Zika Virus Infection in Adults

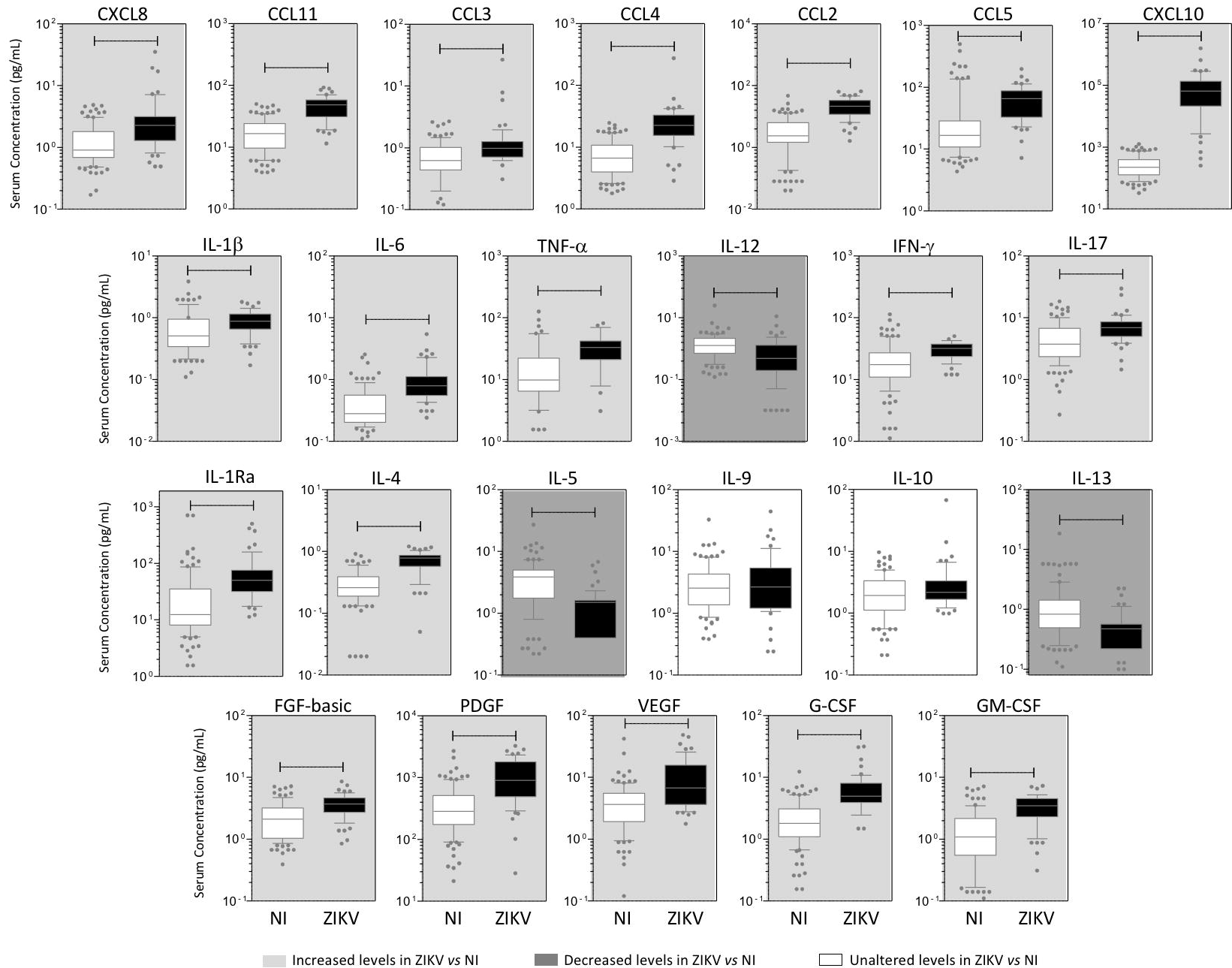


Fig 3. Rhythms of Viremia, Chemokines, Cytokines and Growth Factors Early After Zika Virus Infection in Adults

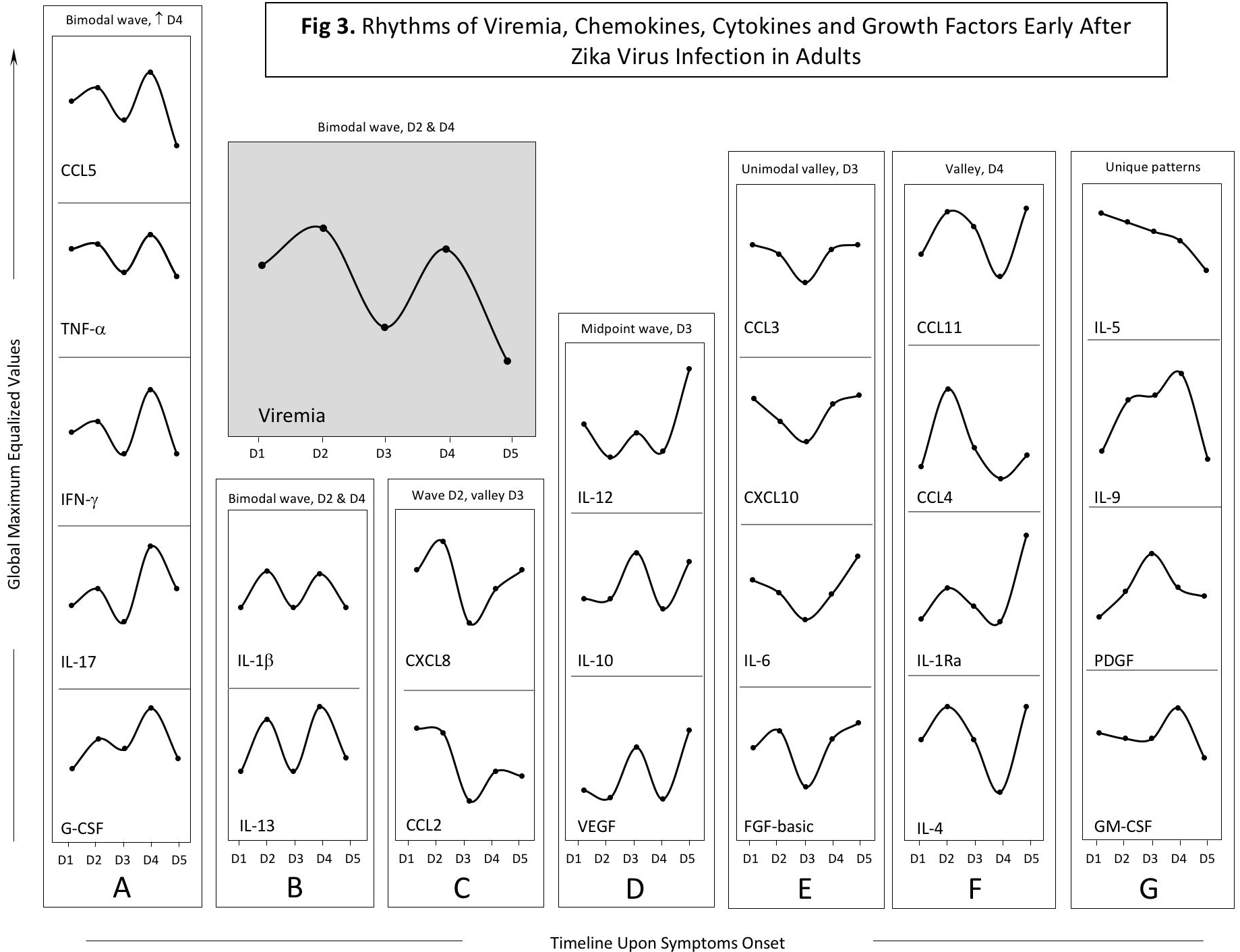
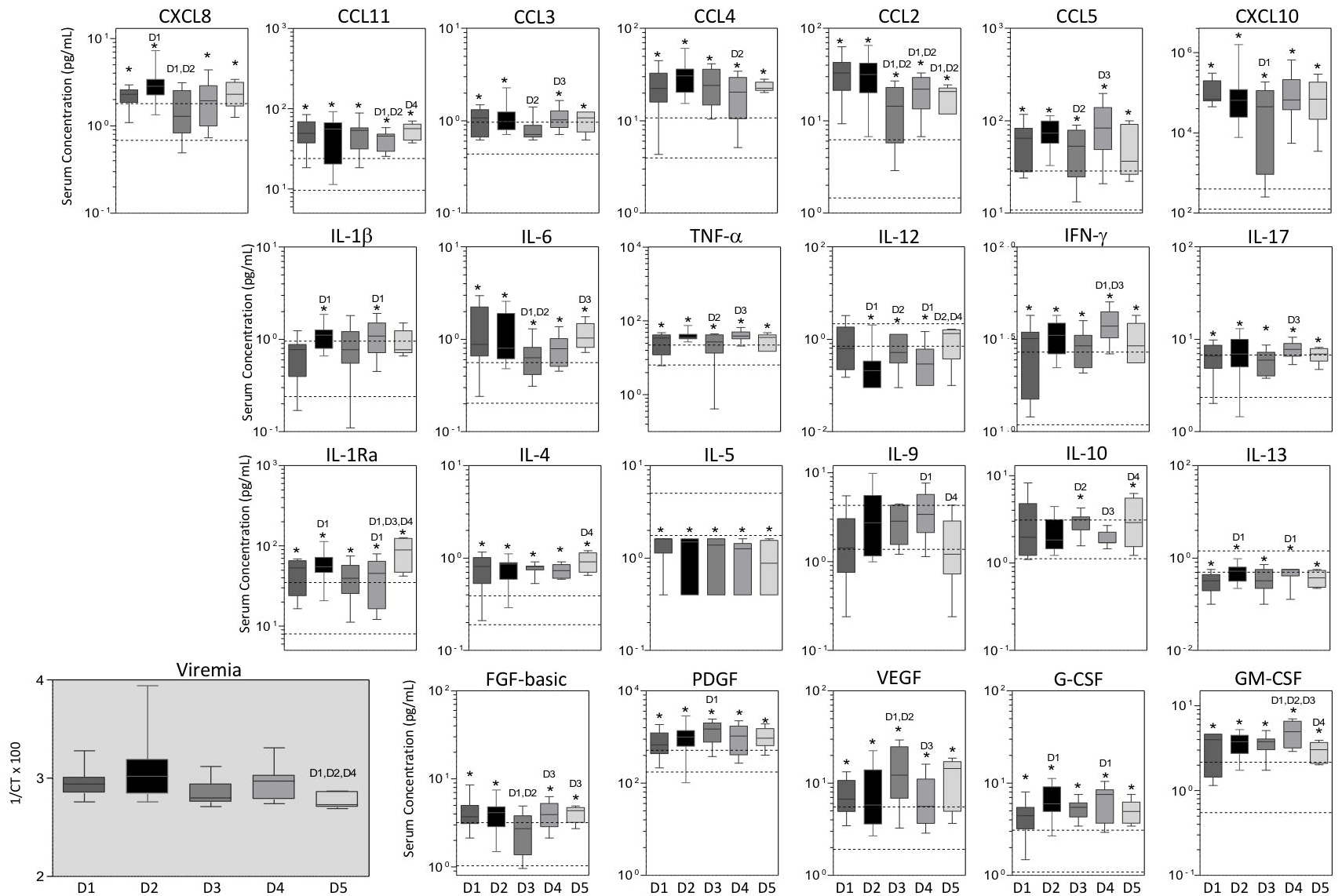


Fig 4. Kinetics of Viremia, Serum Chemokines, Cytokines and Growth Factors Early After Zika Virus Infection in Adults

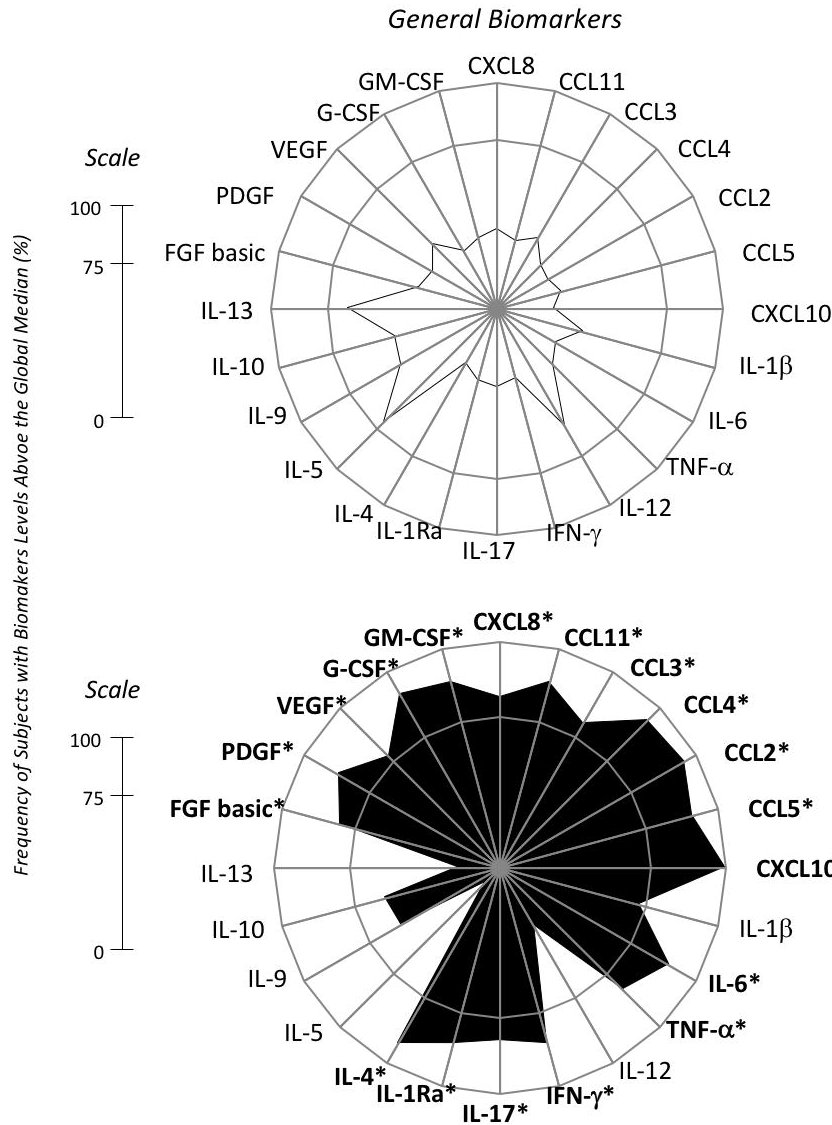


Timeline Upon Symptoms Onset

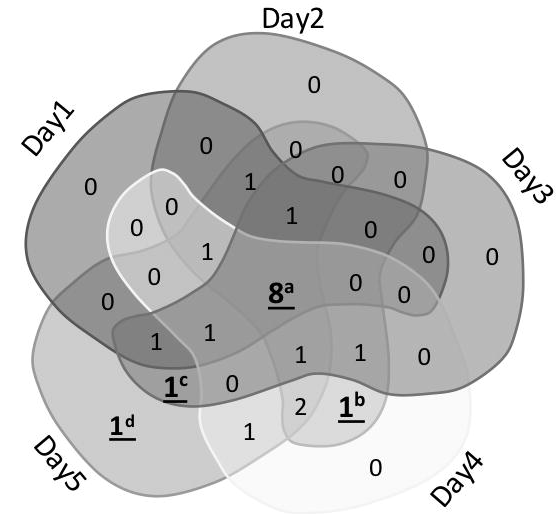
Fig 5. General and Timeline Biomarkers upon Symptoms Onset Early After Zika Virus Infection in Adults

Non-Infected Controls - NI

Zika Virus Infected Patients - ZIKV



Timeline Biomarkers Upon Symptoms Onset



<i>Days of Symptoms</i>	<i>Intersections</i>
<u>ALL^a</u>	<u>CCL4,CCL2,CCL5,CXCL10</u> <u>IL-6, IL-4, PDGF, G-CSF</u>
D1,D2,D3,D5	IL-1Ra
D1,D2,D4,D5	IL-17
D1,D3,D4,D5	CCL11
D2,D3,D4,D5	IFN- γ
D1,D2,D5	CXCL8
D1,D3,D5	VEGF
D2,D3,D4	GM-CSF
D2,D4,D5	CCL3,IL-1 β
<u>D2,D4^b</u>	<u>TNF-α</u>
<u>D3,D5^c</u>	<u>IL-10</u>
D4,D5	FGF-basic
<u>D5^d</u>	<u>IL-12</u>

* Biomarkers with Levels Above the Global Median in >75% of Subjects

Biomarkers Labels: ^a Universal; ^b Peak of Viremia; ^c Valley of Viremia; ^d Late Biomarker

Fig 6. Timeline Biomarker Networks Early After Zika Virus Infection in Adults

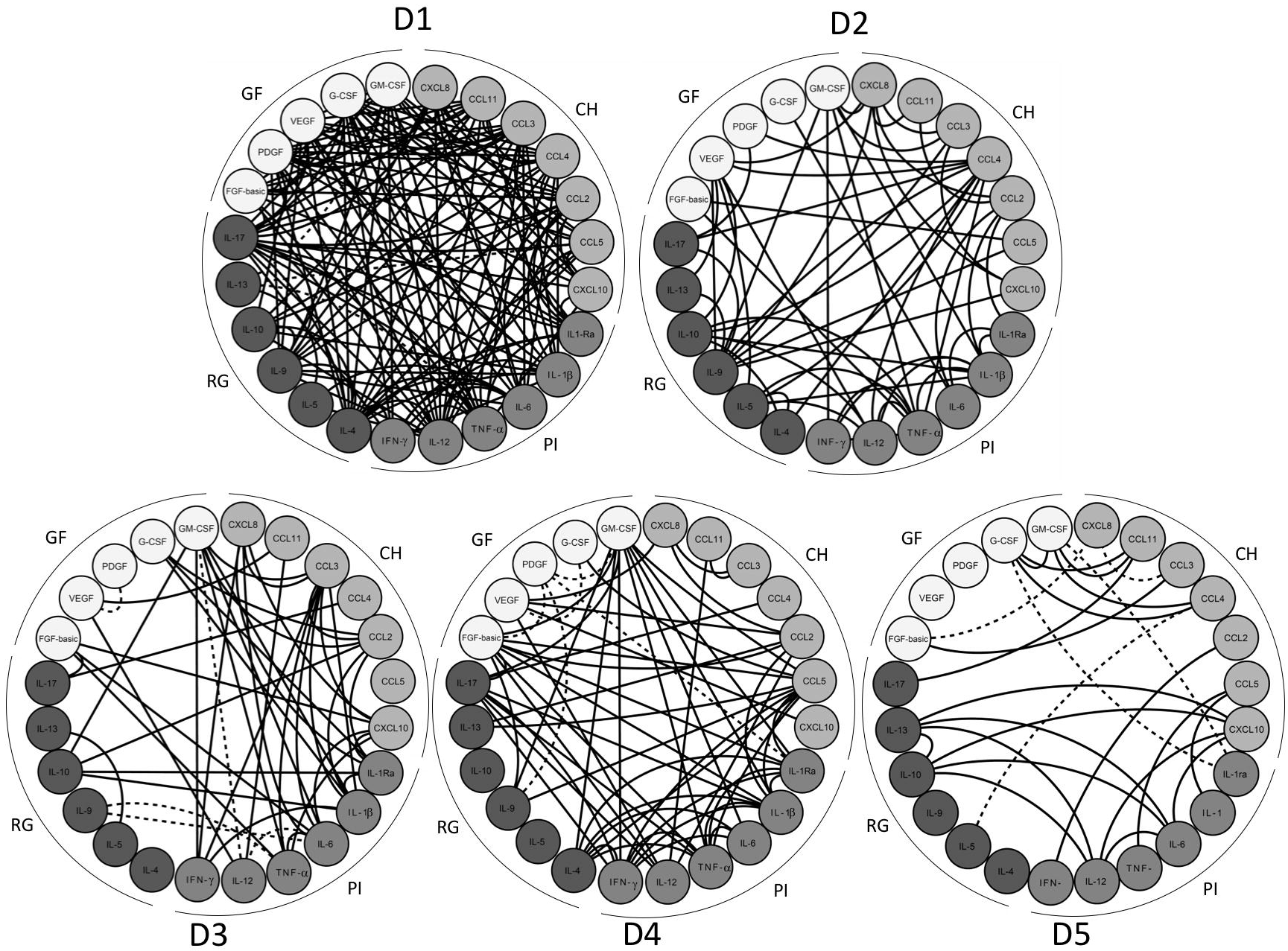
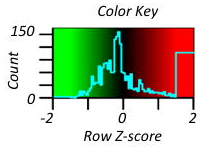
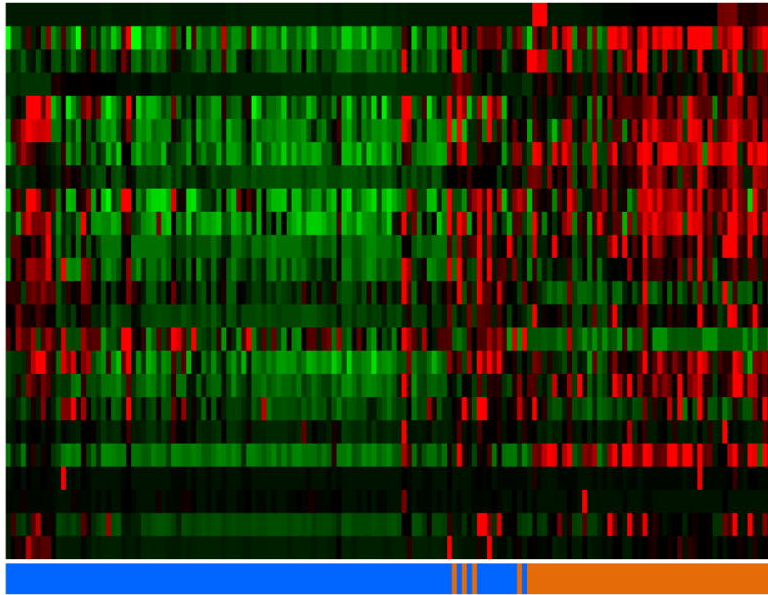


Fig 7. High-dimensional Data Analysis Early After Zika Virus Infection in Adults

Heatmap Assemblage

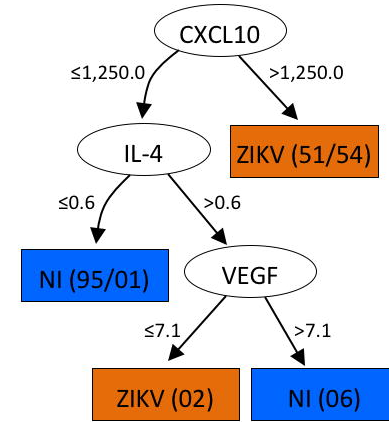


■ NI
■ ZIKV



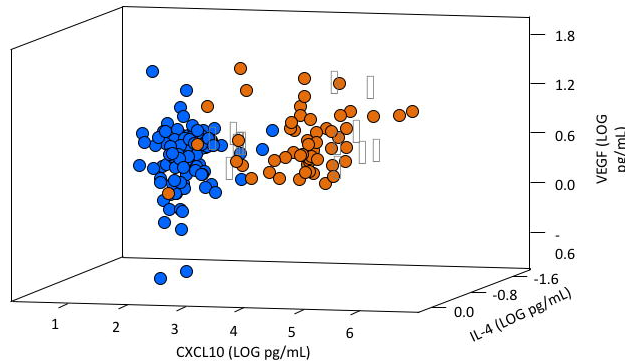
CXCL10
 IL-4
 VEGF
 PDGF
 IFN- γ
 TNF- α
 CCL11
 CCL4
 FGF-basic
 GM-CSF
 IL-6
 IL-1 β
 IL-12
 CXCL8
 IL-5
 IL-17
 G-CSF
 IL-9
 IL-10
 CCL2
 CCL3
 IL-13
 IL-1Ra
 CCL5

Decision Tree Algorithm

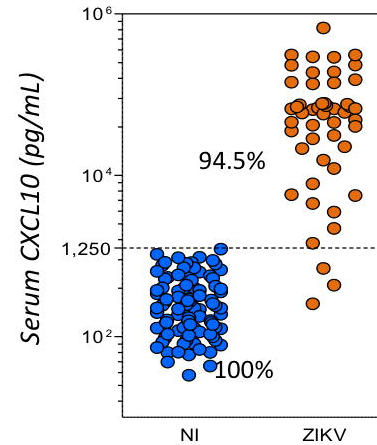


Global Accuracy = 99.4%
 LOOCV = 96.8%

3D-Plot of Major Attributes



Root Attribute Scatter Plot



ROC Curve Analysis

